

REFLECTION OF SEISMIC WAVES  
AT OBLIQUE ANGLES FROM  
DEEP SEA SEDIMENTS.

by

Peter C. Beamish.

SUBMITTED IN PARTIAL FULFILLMENT  
OF THE REQUIREMENTS FOR THE  
DEGREE OF  
MASTER OF SCIENCE

at the

MASSACHUSETTS INSTITUTE OF TECHNOLOGY

April, 1964.

Signature of Author .....  
Department of Geology and Geophysics, April 30, 1964.

Certified by ... / ~~Thesis Advisor~~ / .....

Accepted by .....  
Chairman, Department Committee  
Graduate Students.

✓

REFLECTION OF SEISMIC WAVES  
AT OBLIQUE ANGLES FROM  
DEEP SEA SEDIMENTS.

ABSTRACT

by

Peter C. Beamish.

Submitted to the Department of Geology and Geophysics  
on April 30, in partial fulfillment of the requirement for  
the degree of Master of Science.

The theory of oblique angle seismic reflectivity, as  
applied to oceanographic research, is presented. Recent  
experiments have been performed to measure the reflectivity  
of ocean sediments at oblique angles. Results from the  
Tyrrhenian Sea and from north of Puerto Rico indicate the  
possibility that the sound velocity in the first layer sedi-  
ments is less than the sound velocity of the bottom water.

Thesis Supervisor: John B. Hersey.  
Title: Professor of Oceanography.

TABLE OF CONTENTS

Abstract . . . . .	1
Introduction . . . . .	1
I. Theory of Oblique Reflections at Sea	
I-1 Reflectivity Curves . . . . .	2
I-2 Limitations on Reflectivity Curves. . . . .	9
I-3 Other Considerations	
I-3-a Reflection from a Porous Medium. . . . .	13
I-3-b Reflection from Two Boundaries . . . . .	17
I-3-c Pulse Reflection . . . . .	18
I-3-d Reflection from an Elastic Medium. . . . .	20
II. Experimental Reflectivity	
II-1 The Experiment . . . . .	22
II-2 Discussion of Results. . . . .	24
II-3 Conclusions. . . . .	31
Bibliography . . . . .	32

TABLE OF ILLUSTRATIONS

1. Theoretical Reflectivity for Ocean Sediments . . . .	6
2. Normal Incidence Reflectivity. . . . .	10
3. Angle of Intrromission. . . . .	12
4. Critical Angle . . . . .	12
5. Sediment Velocity against Porosity . . . . .	14
6. Tyrrhenian Sea Navigation. . . . .	25
7. Tyrrhenian Sea Calibration . . . . .	25
8. Tyrrhenian Sea Reflectivity. . . . .	26
9. Puerto Rico Navigation . . . . .	26
10. Puerto Rico Reflectivity 1a. . . . .	28
11. Puerto Rico Reflectivity 1b. . . . .	28
12. Puerto Rico Reflectivity 2a. . . . .	29
13. Puerto Rico Reflectivity 2b. . . . .	29

## Introduction

An experiment has been developed to measure the in situ acoustic properties of ocean sediments. This work outlines the progress and future capabilities of the experiment.

The first part concerns the theory of the reflection of seismic waves at oblique angles from deep sea sediments. A reflectivity equation is developed from which typical amplitude reflectivity curves have been drawn. Limitations to these curves have been developed specifically for cases that would actually exist in oceanographic research. A number of further considerations in the theory have been discussed and many of these may be important in future work in this field.

The second part concerns both the experiment at sea and in the laboratory. The results are presented and discussed in relation to the theoretical ideas developed in part I.

Indebtedness is gratefully acknowledged to Professor John B. Hersey of the Woods Hole Oceanographic Institution and M.I.T. for his encouragement, and support. He has been the chief scientist at sea as well as inventor and promoter of these experiments. Acknowledgement is also made to Professor S.M. Simpson of M.I.T. for advice and guidance and to Don Krotzer and Stan Jacobs for assistance with many of the experimental problems.

# I THEORY OF OBLIQUE REFLECTIONS AT SEA

## I-1 Reflectivity Curves

The equations of motion of an elastic wave in a liquid can be derived by infinitesimal strain theory, directly from Newton's second law. These equations define the propagation of longitudinal vibrations through the medium; transverse vibrations are not defined because of the vanishing of the terms containing rigidity.

The equations are:

$$\begin{aligned} \rho \frac{\partial^2 u}{\partial t^2} &= \lambda \frac{\partial \phi}{\partial x} & (u, v, w) &= \text{displacement vector} \\ \rho \frac{\partial^2 v}{\partial t^2} &= \lambda \frac{\partial \phi}{\partial y} & \rho &= \text{density} \\ \rho \frac{\partial^2 w}{\partial t^2} &= \lambda \frac{\partial \phi}{\partial z} & \lambda &= \text{Lamé constant} \\ & & & \text{or incompressibility } K \\ & & \phi &= \text{dilatation} \\ & & & \text{or } \frac{\partial u}{\partial x} + \frac{\partial v}{\partial y} + \frac{\partial w}{\partial z} \end{aligned}$$

In general  $K = \lambda + \frac{2}{3}\mu$ , but for a liquid the rigidity or shear modulus  $\mu = 0$ .

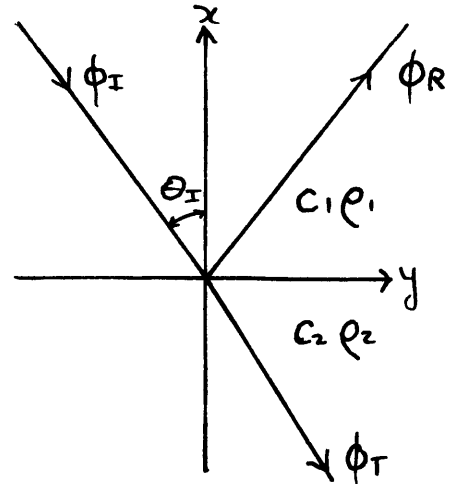
Differentiating with respect to  $\frac{\partial}{\partial x}$ ,  $\frac{\partial}{\partial y}$  and  $\frac{\partial}{\partial z}$  respectively, adding and substituting we obtain:

$$\rho \frac{\partial^2 \phi}{\partial t^2} = K \nabla^2 \phi \quad \nabla^2 = \frac{\partial^2}{\partial x^2} + \frac{\partial^2}{\partial y^2} + \frac{\partial^2}{\partial z^2}$$

which is the wave equation for longitudinal elastic pressure waves in a liquid. The dilatation  $\phi$  is propagated with a velocity  $C = \left(\frac{K}{\rho}\right)^{1/2}$  and the generalized wave equation for a liquid becomes:

$$\frac{\partial^2 \phi}{\partial t^2} = C^2 \nabla^2 \phi \quad (1)$$

Let us consider a two dimensional ocean in which the x-axis is normal to a horizontal sediment boundary and the y-axis lies along the boundary. We assume that the rigidity of the water above the y-axis is zero and that the rigidity of the sediments below is negligible, so that the y-axis becomes



a boundary between two fluids, across which there is a change in sound velocity  $C$ , and density  $\rho$ . The case of negligible rigidity in surface sediments is considered to exist in a number of ocean areas (Urlick, 1947; Hamilton, 1956). The possibility of the existence of shear waves, however, will be discussed in a later section.

Let:

$$\begin{aligned}\phi_I &= \text{incident displacement} \\ \phi_R &= \text{reflected displacement} \\ \phi_T &= \text{transmitted displacement}\end{aligned}$$

The general solution of the wave equation (1) for one-dimensional motion along the x-axis is:

$$\phi = f(x-ct) + g(x+ct)$$

where  $f$  and  $g$  are arbitrary functions depending on the initial and boundary conditions.

Let us consider a simple harmonic wave in the x-y plane. To solve the wave equation we need merely to

substitute sine or cosine functions for the arbitrary functions in the general solution and to resolve the ray path in the x and y directions. The simple harmonic solution is thus of the form:

$$\phi = A e^{i\psi(t,x,y)}$$

where A is the amplitude and  $\psi(t,x,y)$  is the argument of the resultant pressure wave. The displacement potentials  $\phi_I$ ,  $\phi_R$  and  $\phi_T$  can then be written:

$$\begin{aligned}\phi_I &= A e^{i\psi_I(t,x,y)} \\ \phi_R &= B e^{i\psi_R(t,x,y)} \\ \phi_T &= C e^{i\psi_T(t,x,y)}\end{aligned}\tag{2}$$

Boundary conditions between the two media are:

1. continuity of vertical particle velocity, and
2. continuity of pressure

which in terms of displacement potentials, become:

$$\frac{\partial \phi_I}{\partial x} + \frac{\partial \phi_R}{\partial x} = \frac{\partial \phi_T}{\partial x}\tag{3}$$

$$\rho_1 \frac{\partial \phi_I}{\partial t} + \rho_1 \frac{\partial \phi_R}{\partial t} = \rho_2 \frac{\partial \phi_T}{\partial t}\tag{4}$$

It is required to find the ratio of the amplitude of the reflected wave B to that of the incident wave A, which is by definition the amplitude reflectivity R. By substitution of equations (2) into the equations for the boundary conditions (3) and (4) we obtain two equations

containing the three unknown amplitudes  $A$  ,  $B$  and  $C$  .  
By eliminating  $C$  we can obtain the required amplitude reflectivity (or Rayleigh reflection coefficient), for plane waves reflected from a plane boundary between two fluids of densities  $\rho_1$  and  $\rho_2$  and sound velocities  $C_1$  and  $C_2$  .

The expression is:

$$R = \frac{\rho_2 \cos \theta_I - \rho_1 \sqrt{(C_1/C_2)^2 - \sin^2 \theta_I}}{\rho_2 \cos \theta_I + \rho_1 \sqrt{(C_1/C_2)^2 - \sin^2 \theta_I}} \quad (5) \quad 1.$$

where  $\theta_I$  is the angle of incidence of the plane wave on the boundary.

Examples of theoretical reflectivity curves for typical ocean sediments have been drawn in Figure 1. If the sound velocity of the sediments ( $C_2$ ) is greater than the sound velocity of the overlying water layer ( $C_1$ ), then the reflectivity will increase from normal incidence to unity (total reflection) at the critical angle  $\theta_c = \sin^{-1} \frac{C_1}{C_2}$  , since at this angle the radicals in the reflectivity expression vanish. Beyond this angle of incidence the radicals become imaginary and they may be expressed by  $-i \sqrt{\sin^2 \theta_I - (C_1/C_2)^2}$  . Thus the reflectivity expression for  $\theta_I > \theta_c$  becomes:

$$R = \frac{\rho_2 \cos \theta_I + i \rho_1 \sqrt{\sin^2 \theta_I - (C_1/C_2)^2}}{\rho_2 \cos \theta_I - i \rho_1 \sqrt{\sin^2 \theta_I - (C_1/C_2)^2}}$$

1. For a detailed derivation of this equation see Introduction to the Theory of Sound Transmission by C. B. Officer, McGraw-Hill Inc. 1958.



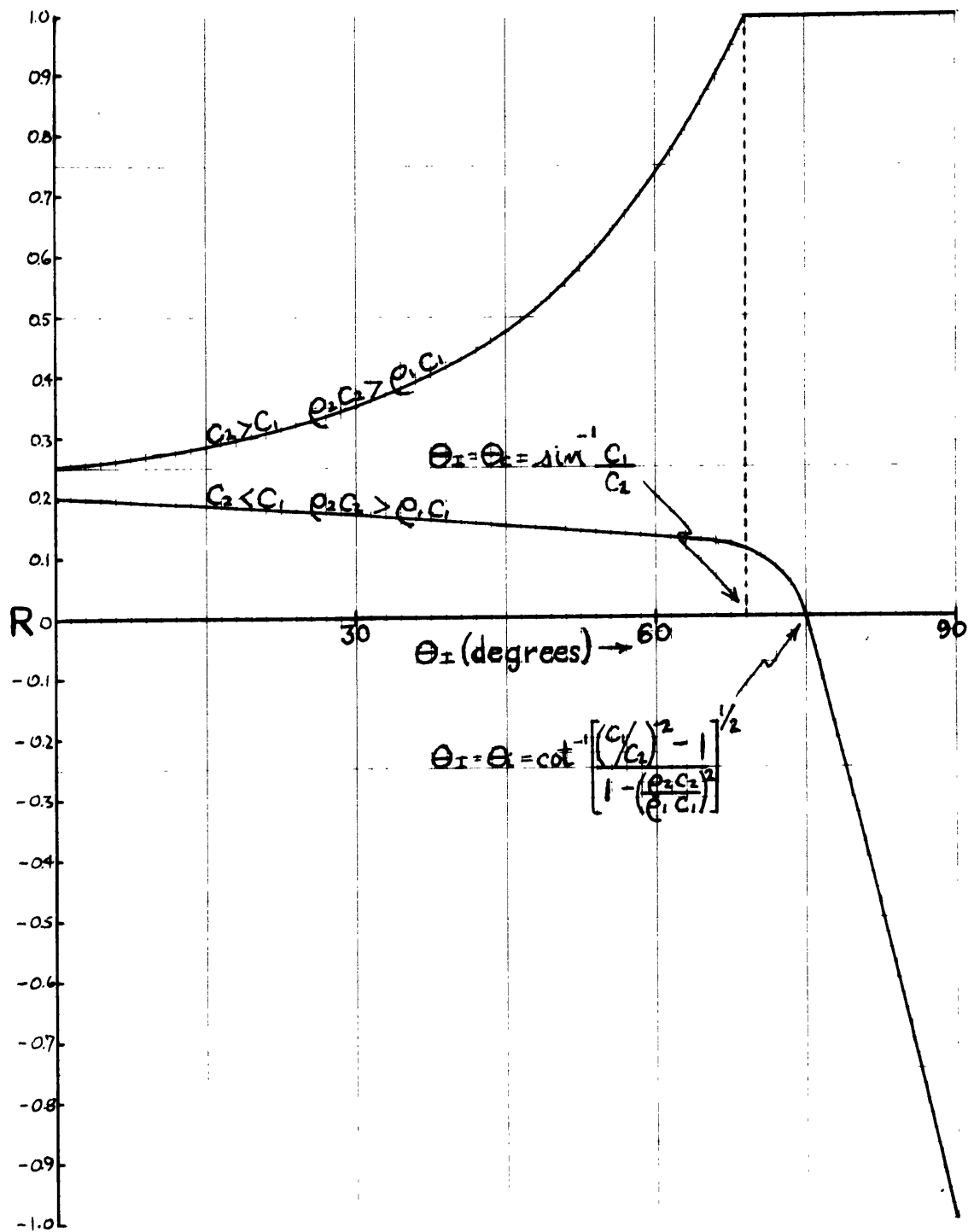


FIGURE I

Rationalizing the denominator, and separating into real and imaginary parts, we get:

$$R = \frac{\rho_2^2 \cos^2 \theta_I + 2i\rho_1\rho_2 \cos \theta_I \sqrt{\sin^2 \theta_I - (c_1/c_2)^2} - \rho_1^2 [\sin^2 \theta_I - (c_1/c_2)^2]}{\rho_2^2 \cos^2 \theta_I + \rho_1^2 [\sin^2 \theta_I - (c_1/c_2)^2]}$$

$$= \frac{\rho_2^2 \cos^2 \theta_I - \rho_1^2 [\sin^2 \theta_I - (c_1/c_2)^2]}{\rho_2^2 \cos^2 \theta_I + \rho_1^2 [\sin^2 \theta_I - (c_1/c_2)^2]} + i \frac{2\rho_1\rho_2 \cos \theta_I \sqrt{\sin^2 \theta_I - (c_1/c_2)^2}}{\rho_2^2 \cos^2 \theta_I + \rho_1^2 [\sin^2 \theta_I - (c_1/c_2)^2]}$$

If we let  $\epsilon$  be the phase change of the reflected wave with respect to the incident wave then  $R = e^{i\epsilon} = \cos \epsilon + i \sin \epsilon$ . Substituting for  $\cos \epsilon$  and  $\sin \epsilon$  we obtain:

$$\tan \epsilon = \frac{\sin \epsilon}{\cos \epsilon} = \frac{2\rho_1\rho_2 \cos \theta_I \sqrt{\sin^2 \theta_I - (c_1/c_2)^2}}{\rho_2^2 \cos^2 \theta_I - \rho_1^2 [\sin^2 \theta_I - (c_1/c_2)^2]}$$

$$\text{or } \epsilon = \tan^{-1} \frac{2\rho_1\rho_2 \cos \theta_I \sqrt{\sin^2 \theta_I - (c_1/c_2)^2}}{\rho_2^2 \cos^2 \theta_I - \rho_1^2 [\sin^2 \theta_I - (c_1/c_2)^2]}$$

Thus for  $\theta > \theta_c$  the amplitude of the reflected wave remains unity but the phase change  $\epsilon$  is 0 degrees at  $\theta = \sin^{-1} \frac{c_1}{c_2}$  and increases to 180 degrees at  $\theta = 90$  or grazing incidence.

If the sound velocity of the sediments is less than the sound velocity of the overlying water layer, then as  $\theta_I$  increases the numerator of the reflectivity expression decreases less rapidly than the denominator and the reflectivity decreases. The reflectivity becomes zero at  $\theta_i$  the angle of intromission which may be solved for as follows.

From the reflectivity expression for  $R=0$ :

$$\rho_2 \cos \theta_i = \rho_1 \sqrt{(c_1/c_2)^2 - \sin^2 \theta_i}$$

$$\rho_2^2 \cos^2 \theta_i = \rho_1^2 \frac{c_1^2}{c_2^2} - \rho_1^2 \sin^2 \theta_i$$

$$\rho_1^2 \sin^2 \theta_i + \rho_2^2 \cos^2 \theta_i = \rho_1^2 \frac{c_1^2}{c_2^2} (\sin^2 \theta_i + \cos^2 \theta_i)$$

$$\frac{\cos^2 \theta_i}{\sin^2 \theta_i} = \frac{\rho_1^2 - \rho_1^2 \frac{c_1^2}{c_2^2}}{\rho_1^2 \frac{c_1^2}{c_2^2} - \rho_2^2}$$

$$\cot^2 \theta_i = \frac{\rho_1^2 (1 - \frac{c_1^2}{c_2^2})}{\frac{c_1^2}{c_2^2} \rho_1^2 - \rho_2^2} \quad c_1 \neq 0$$

$$\theta_i = \cot^{-1} \left[ \frac{(c_1/c_2)^{-2} - 1}{1 - \left( \frac{\rho_2 c_2}{\rho_1 c_1} \right)^2} \right]^{1/2} \quad \rho_1 \neq 0$$

Beyond the angle of intromission the sign of the reflectivity becomes negative, indicating a 180 degree phase shift of the reflected wave relative to the incident wave. The reflectivity increases to a value of unity for  $\theta = 90^\circ$ .

Limitations on Reflectivity Curves

It now becomes important to discuss limitations on the reflectivity curves for oceanographic experiments. The most important limitation is on the ordinate intercepts or reflectivities at normal incidence. These intercepts will be important in determining initial slopes of the curves.

For  $\Theta=0$  the amplitude reflectivity of equation (5) reduces to:

$$R = \frac{\rho_2 c_2 - \rho_1 c_1}{\rho_2 c_2 + \rho_1 c_1}$$

In order to understand the dependence of  $R$  on the acoustic properties of the sediment surface we have plotted the reflectivity at normal incidence against the velocity ratio  $c_1/c_2$  (Figure 2).

According to the emulsion theory of Wood (1941, p.361), a lower limit on  $c_2$  is predicted to be about 3% less than that of water. This prediction is in agreement with measurements of sediment sound velocities in the Pacific reported by Fry and Raitt (1961, pp.593-595). Thus the maximum velocity ratio  $c_1/c_2$  will be 1.03. To prevent overturning, the minimum density ratio  $\rho_2/\rho_1$  is 1.0. Densities in deep sea sediments have been measured by Shumway (1960) in the Pacific and by Laughton (1957) and Sutton, Berckheimer, and Nafe (1957) in the Atlantic and values generally fall within the range 1.3-1.6.

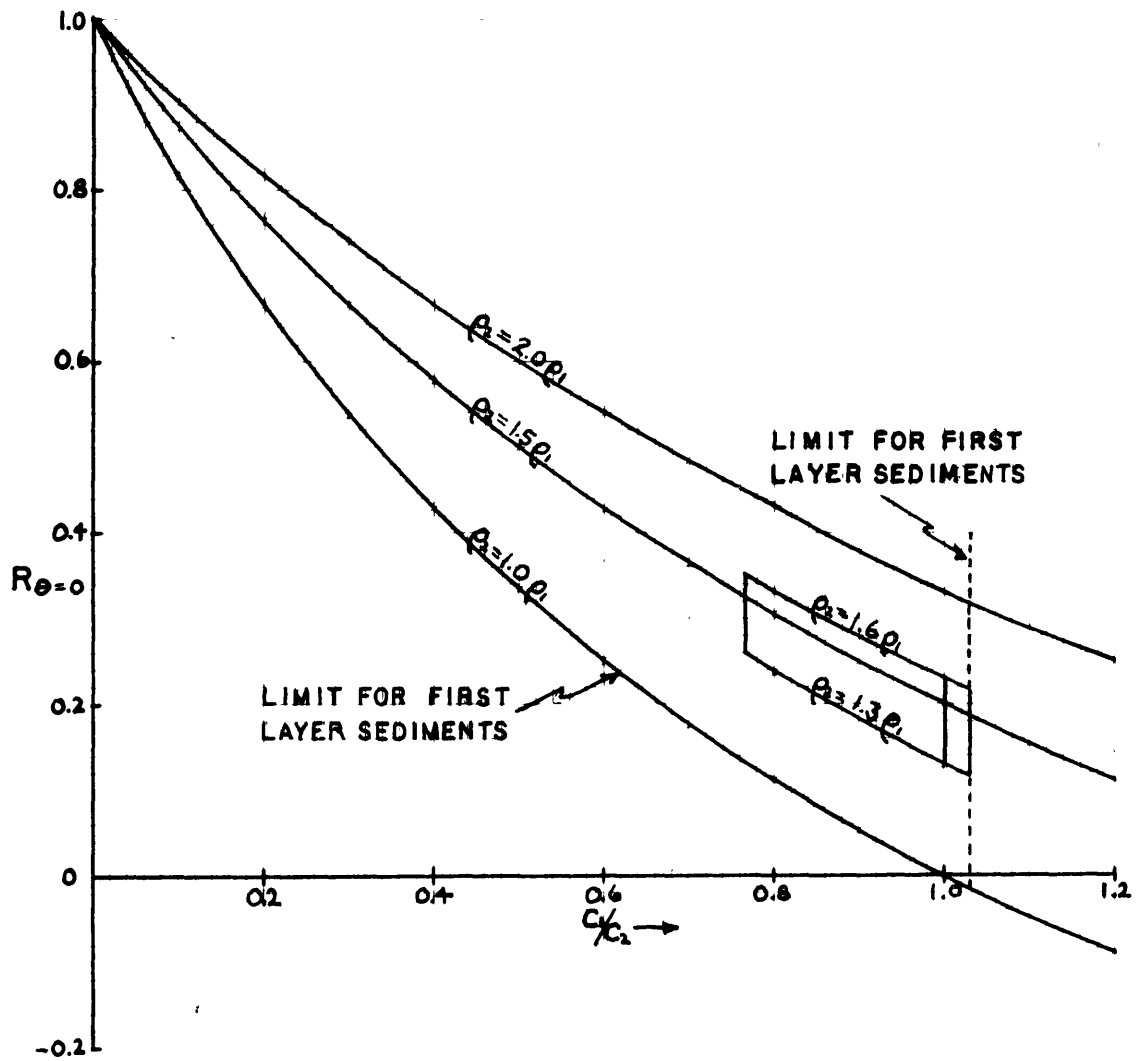


FIGURE 2  
after Ewing, Jardetzky and Press (1957), p.80

We can thus conclude from Figure 2 that normal incidence reflectivities for a velocity inversion layer ( $C_2 < C_1$ ) fall in the range 0.12-0.23 . If we assume  $C_2 > C_1$  and  $C_2 < 2.0$  kilometers per second then the normal incidence reflectivities fall in the range 0.13-0.35 . The only remote possibility for a negative normal incidence reflectivity is for the case  $C_2 < C_1$  and  $\rho_2$  very close to  $\rho_1$  .

Figure 3 shows the variation of the angle of intromission with sediment density ( $\rho_1 = 1.03$  grams per cc.). The curve  $C_2 = 0.97 C_1$  is considered to represent the limiting case for first layer sediments. As  $C_1$  approaches  $C_2$ , the curves approach the asymptotes  $\theta_i = 90$  degrees and  $\rho_2 = 1.03$  . In the limit of continuity of acoustic impedance ( $\rho_2 C_2 = \rho_1 C_1$ ),  $\theta_i = 0$ . For a practical range of sediment density of 1.3-1.6 the angle of intromission varies from 70-90 degrees depending on the velocity contrast.

Figure 4 shows the variation of critical angle with sediment sound velocity ( $C_1 = 1.55$  kilometers per second). As  $C_2$  increases,  $\theta_c$  decreases from 90 degrees and its rate of decrease falls off very rapidly. For a practical limit of 2.0 kilometers per second for  $C_2$ , the critical angle would be 51 degrees.

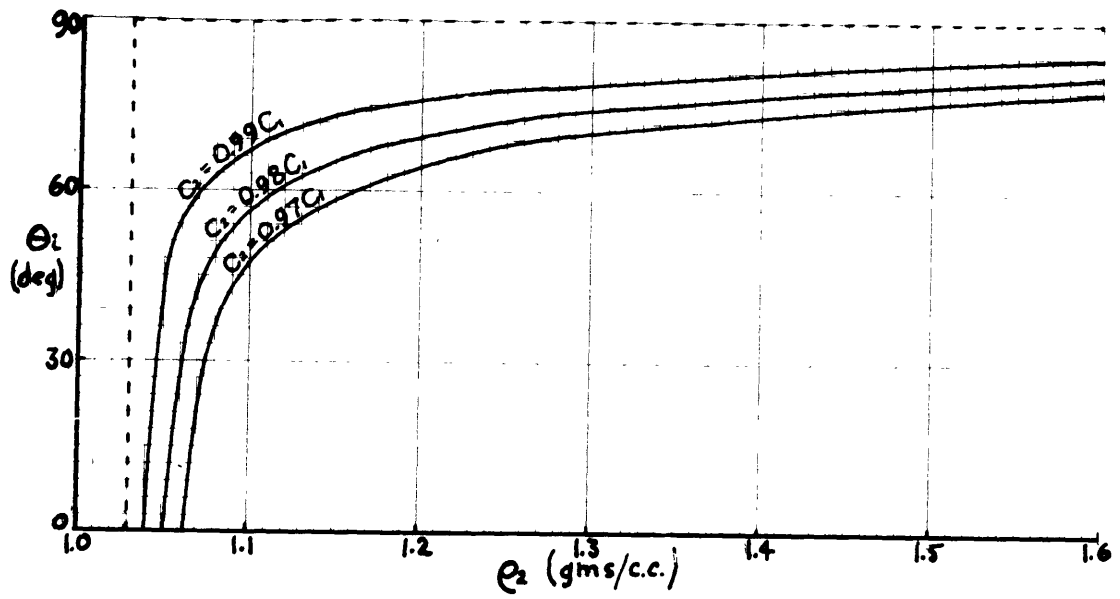


FIGURE 3

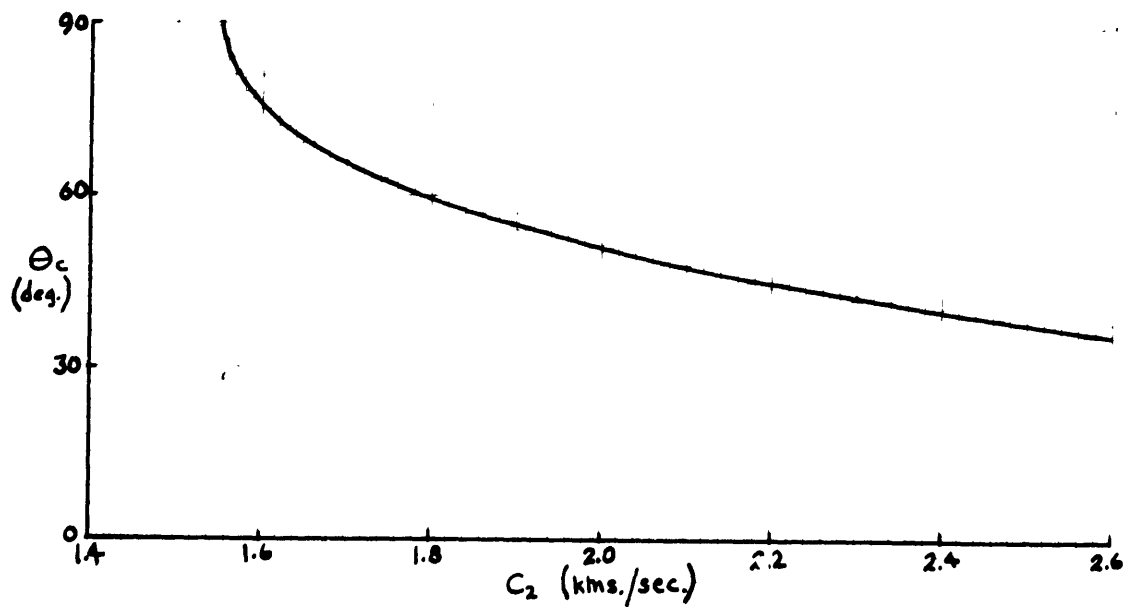


FIGURE 4

I-3

Other Considerations

I-3-a

Reflections from a Porous Medium

Sediments on the ocean floor consist of both particulate matter and a pore-filling fluid. It has been discovered both theoretically and experimentally that the sound velocity of a mixture can be lower than the individual sound velocities of either of its components.

Urick (1947) has determined the sound velocity in an ideal mixture of two components. He has assumed that the medium has no rigidity and no viscosity, which approximates the case for a suspension of a solid component in a fluid. The sound velocity of such a mixture is given by:

$$C_2 = [g\rho_1 + (1-g)\rho_s]^{1/2} [g/\rho_1 C_1^2 + (1-g)/\rho_s C_s^2]^{-1/2} \quad (6)$$

where  $\rho_1$  and  $C_1$  are the density and sound velocity of the fluid,  $\rho_s$  and  $C_s$  are the density and sound velocity of the solid, and  $g$  is the porosity, or ratio of the volume fraction of fluid to total volume.

For  $g = 1$  (all fluid) equation (6) reduces to  $C_1$ , and for  $g = 0$  (all solid) the equation reduces to  $C_s$ . In ocean sediments  $\rho_s > \rho_1$  and  $C_s > C_1$ . As the porosity of the mixture is decreased from unity, the velocity of the mixture will decrease from  $C_1$ , until the  $(1-g)$  terms become dominant, when the velocity will increase to  $C_s$ . Figure 5 is a plot of equation (6).

Hamilton (1956) has computed experimental curves for



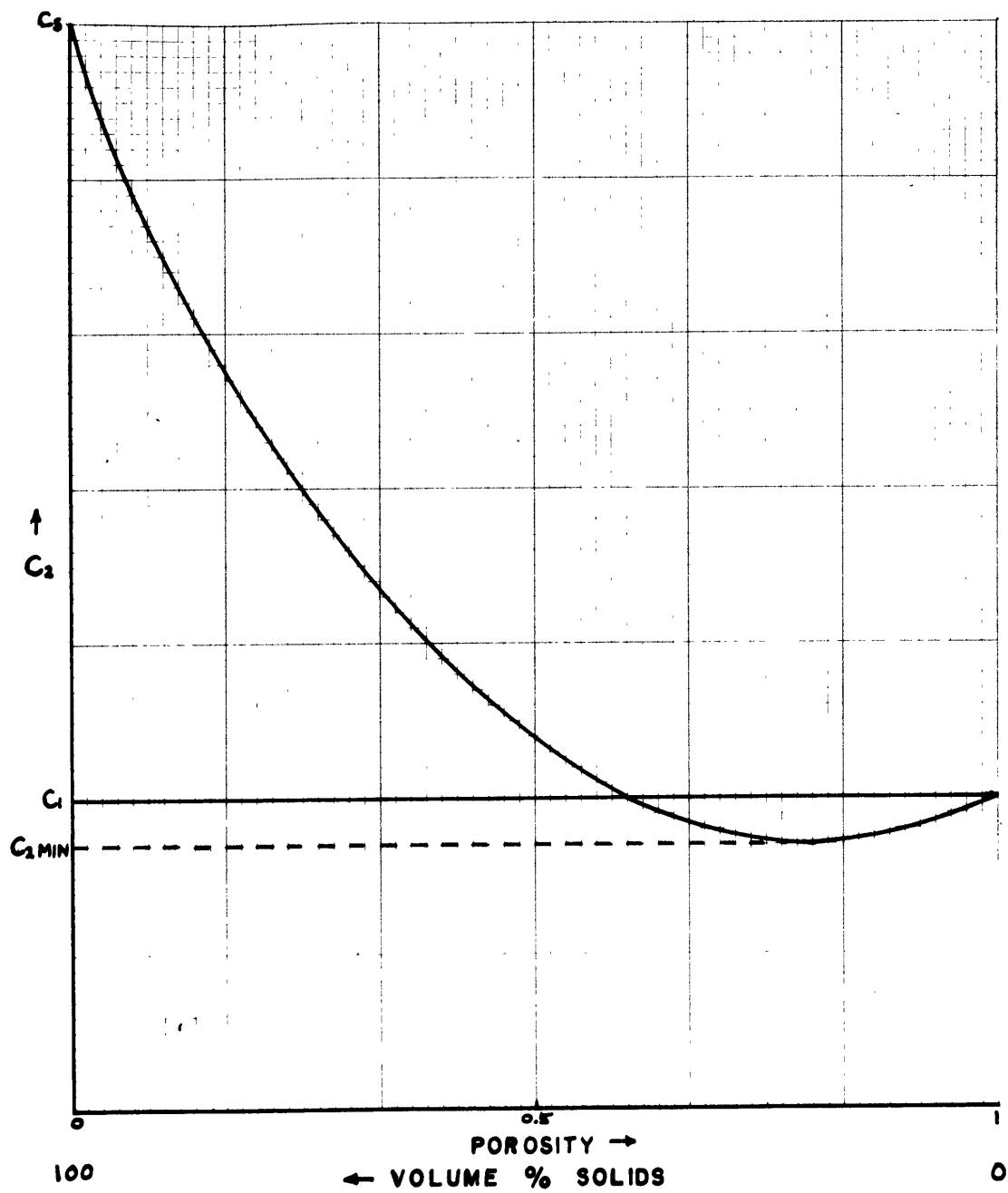


FIGURE 5

after Officer (1958), p.259

$C_2$  as a function of porosity for suspensions in sea water of incompressible particles, quartz particles, and particles of a typical sand-silt off San Diego. He has found that the minimum sound velocity for the sand-silt occurs at a porosity of approximately 0.78 . The corresponding porosities for the incompressible and quartz particles were slightly higher. Minimum sound velocity (  $C_{2\text{MIN}}$  ) has been predicted by Wood (1941) to be about 3% less than that of water (  $C_1$  ) which corresponds with experimental results of Fry and Raitt (1961).

In order to explain the phenomenon described by Figure (6) we must recall that the sound velocity of a fluid medium is equal to  $(K/\rho)^{1/2}$  where  $K$  is the bulk modulus or incompressibility and  $\rho$  is the density. The effect of adding particulate matter to sea water is first to increase the density without appreciably changing the bulk modulus, thus decreasing the sound velocity.

The conditions under which velocity inversion (  $C_2 < C_1$  ) can be measured in a real sediment have become somewhat controversial. Sediments may have some rigidity or viscosity so that the assumptions made in equation (6) are approximations for specific cases only.

There are three effects which can obscure the interpretation of a velocity inversion layer in the ocean.

#### 1. The Viscous Effect

This effect is concerned with the motion of the fluid within the pore spaces. Its magnitude is inversely

proportional to both the size of the pore spaces and the interconnections between pores. As the viscous effect increases, so does both the dispersion and attenuation of sound waves in the sediment. Both dispersion and attenuation are directly proportional to the acoustic frequency.

### 2. Sub-bottom Reflections

This effect is that acoustic sub-bottom returns influence bottom returns because of a difficulty in time resolution. The superposition of the reflected amplitudes and phases may obscure the interpretation of the velocity inversion.

### 3. Velocity Gradient Effect

If a positive velocity gradient exists within the sediment layer, sound energy is refracted upward and interferes with the surface arrival (Hill, 1952). The reflection coefficient  $R$  becomes complex and both its amplitude and phase are dependent on frequency.

Officer (1958 p.215) has placed much emphasis on the viscosity effect but Fry and Raitt (1961 p.595) consider the velocity gradient and sub-bottom effects to be far more important in obscuring velocity inversion. According to Officer, a high porosity sediment can have a sound velocity lower than that of the contained fluid at low frequencies but higher at high frequencies. However, Laughton (1957 p.253) has shown that the sound frequency must be increased to 150 megacycles to obtain a 1% change in sound velocity. The existence of dispersion in first layer ocean sediments is therefore somewhat doubtful.

I-3-b

Reflection from Two Boundaries

Officer (1958) has derived a reflectivity expression for the reflection of a sound wave from both a bottom and sub-bottom boundary. The major differences from the reflectivity expression derived earlier are a dependence on frequency of the incident wave train as well as a dependence on thickness of the first sedimentary layer.

The reflectivity shows a series of maxima and minima as a function of frequency, at any particular angle of incidence. The frequencies and amplitudes of the maxima and minima will change with the angle of incidence. Therefore for any particular frequency, the reflectivity will show a series of maxima and minima as a function of the angle of incidence.

For sound waves travelling from a source near the surface of the ocean the incident amplitude will exhibit a series of maxima and minima as a result of surface interference as well as a general attenuation of the higher frequencies as a result of absorption. To these maxima and minima will be added those of the layering effect described above and a third set will be added due to surface interference at the receiver. In all three cases the maxima and minima will be dependent on the angle of incidence and the resulting reflectivity curve will show a complicated series of maxima and minima dependent on the frequency, as the angle of incidence increases.

I-3-c

Pulse Reflection

We have until now, been considering the reflection of a simple harmonic plane wave. It will be important to describe reflectivity differences for a pulse of waves.

A pulse may be considered as consisting of a continuous spectrum of individual frequencies each with a specified amplitude and phase. If a simple harmonic wave is reflected with a phase shift that is independent of frequency, we may therefore expect a pulse, under the same conditions, to be reflected with a change in shape.

We have shown that for reflection of a simple harmonic wave from a higher sound velocity medium ( $C_2 > C_1$ ), there is no phase change at angles of incidence steeper than the critical angle. However, at angles of incidence more grazing than the critical angle, there is a phase change of the reflected wave with respect to the incident wave, which increases from 0 degrees at the critical angle to 180 degrees at grazing incidence. We may therefore expect a pulse to change shape at angles of incidence beyond the critical angle.

Arons and Yennie (1950, pp.231-237) have calculated the expected shapes of exponentially decaying shock waves, reflecting from a medium of higher sound velocity ( $C_2 > C_1$ ). For a phase shift of  $\pi$  (grazing incidence), the reflected wave is simply an inverted image of the incident wave, as though the reflection were taking place at a free surface. There is no distortion.

For the reflection of a simple harmonic wave from a lower sound velocity medium (  $C_1 > C_2$  ), there is a phase change of  $\pi$  at and beyond the angle of intromission and thus a pulse will merely be inverted and will not change shape for this case.

It is important to note, however, that despite a distortion of the shape of a pulse, the distribution of energy in the Fourier spectrum remains unaltered upon reflection (Arons and Yennie, 1950).

I-3-d

Reflection from an Elastic Medium

In part I-1 we discussed reflectivity for a plane wave incident on a plane boundary between two liquids. Let us consider the consequences when the rigidity of the lower layer cannot be neglected.

For the lower layer to have elastic properties, the porosity will be well below the limit for velocity inversion given by Figure 5, and we may expect an increase in both sound velocity and acoustic impedance ( $\rho c$ ) with depth.

As a result of finite rigidity, shear waves will be propagated in the elastic medium. The velocity of these waves ( $\beta$ ) will always be less than that of the longitudinal waves ( $C_2$ ) in the same medium.

Officer (1958) has derived the reflectivity equation for a simple harmonic wave reflected from an elastic medium. The critical angle for longitudinal waves ( $\theta_c$ ) continues to be  $\sin^{-1} c_1/c_2$  while the critical angle for shear waves ( $\theta_\beta$ ) becomes  $\sin^{-1} c_1/\beta$ . Since  $C_2$  is greater than  $\beta$ ,  $\theta_\beta$  will always be greater than  $\theta_c$ .

Two cases exist, one for  $\beta < C_1$  and a second for  $\beta > C_1$ . In both cases the reflectivity increases as the angle of incidence increases from normal incidence to the critical angle  $\theta_c$ . Beyond this critical angle there will be no refracted longitudinal waves in the lower medium but there will be shear waves. Thus the reflectivity decreases

from  $\theta_c$ . If  $\beta > c_1$  there will be no refracted shear waves beyond  $\theta_\beta$ . The reflectivity will increase to unity at  $\theta_\beta$  and there will be total reflection for  $\theta_\beta < \theta < 90^\circ$ . If  $\beta < c_1$ , reflected shear waves will continue in the lower medium until the angle of incidence is such that poor coupling of incident to refracted waves reduces their intensity. The reflectivity will decrease from the critical angle  $\theta_c$  in proportion to the amount of energy lost to the lower medium in shear waves.

Thus the reflectivity curves are essentially the same as for the negligible rigidity case of  $c_2 > c_1$  and  $\rho_2 c_2 > \rho_1 c_1$ , excepting that reflectivity decreases at angles of incidence more grazing than the critical angle  $\theta_c$  and increases again to unity for the case  $\beta > c_1$  at the critical angle  $\theta_\beta$ .



## II EXPERIMENTAL REFLECTIVITY

### II-1 The Experiment

Initial oblique reflectivity experiments were performed near the island of Madeira in the fall of 1961, on board the Research Vessel Chain. Following a number of technical improvements, the experiments were repeated on the same cruise, east of Sardinia in the Tyrrhenian Sea.

Continuous oblique reflection profiles were made in each area by towing an acoustic source behind the ship and listening with a hydrophone suspended beneath a free-floating radio buoy. The source produced high energy acoustic signals at a repetition rate of several seconds. Information received at the hydrophone was transmitted to the ship and recorded on two-channel magnetic tape. A constant voltage calibration pulse, transmitted periodically with the signals, was added to the Tyrrhenian Sea experiment.

A third set of profiles was made on board Chain in December of 1962 north of Puerto Rico. In all experiments, deep-sea areas with minimum topographic relief were chosen, for reason that an underlying purpose has been to find out as much as possible about the acoustic properties of deep sediment ponds.

Apparatus was assembled in the geophysics laboratories at M.I.T. for the purpose of analysing the magnetic tapes. Outputs from the tape recorder were filtered to obtain a maximum signal-to-noise ratio and a filtered amplitude-time

function was recorded on one channel of a high speed graphical pen recorder. A second filtered signal was the input to an analog computer where it was squared and integrated with respect to time, and the resulting energy-time step function was then recorded on a second channel of the graphical recorder. The bottom reflected amplitude-time function had such a great variation in peak amplitude that the integration was an important requisite. Furthermore, the change in shape of the acoustic pulse at angles more grazing than the critical angle, will not influence the integrated measurements (see part I-3-c).

Frequency response curves showed that a maximum signal-to-noise ratio for bottom reflections could be obtained with a high cut-off of 600 cycles per second. The frequency maximum of signals was generally around 100 cycles.

II-2

Discussion of Results

Bottom reflected energies have been plotted against the angle of incidence for one profile in the Tyrrhenian Sea and for four profiles north of Puerto Rico. In the Tyrrhenian Sea the range on the buoy was decreased from 5.5 kilometers to 0.5 kilometers in a water depth of 1800 fathoms (Figure 6). North of Puerto Rico the Chain opened and closed range twice with a maximum range of 15.5 kilometers, in a water depth of 3000 fathoms (Figure 9). The signal-to-noise ratio is unusually low at the higher ranges of the fourth profile so that bottom energies could only be recorded to a maximum range of 13.0 kilometers.

Energy reflectivities of the bottom surface can be calculated from a plot of bottom energy against angle of incidence. The measured bottom energies are first corrected for changes in radio transmission output. A plot of calibration pulse energy against angle of incidence, such as in Figure 7 (for the Tyrrhenian Sea) illustrates the transmission attenuation with range, and from such a graph, a correction factor has been determined for each bottom reflected signal.

Energies of bottom reflected signals received at the hydrophone are proportional to both the source energy and the reflectivity of the bottom, and are inversely proportional to the square of the ray path distance. The source energy may be calculated from 1.) the received bottom

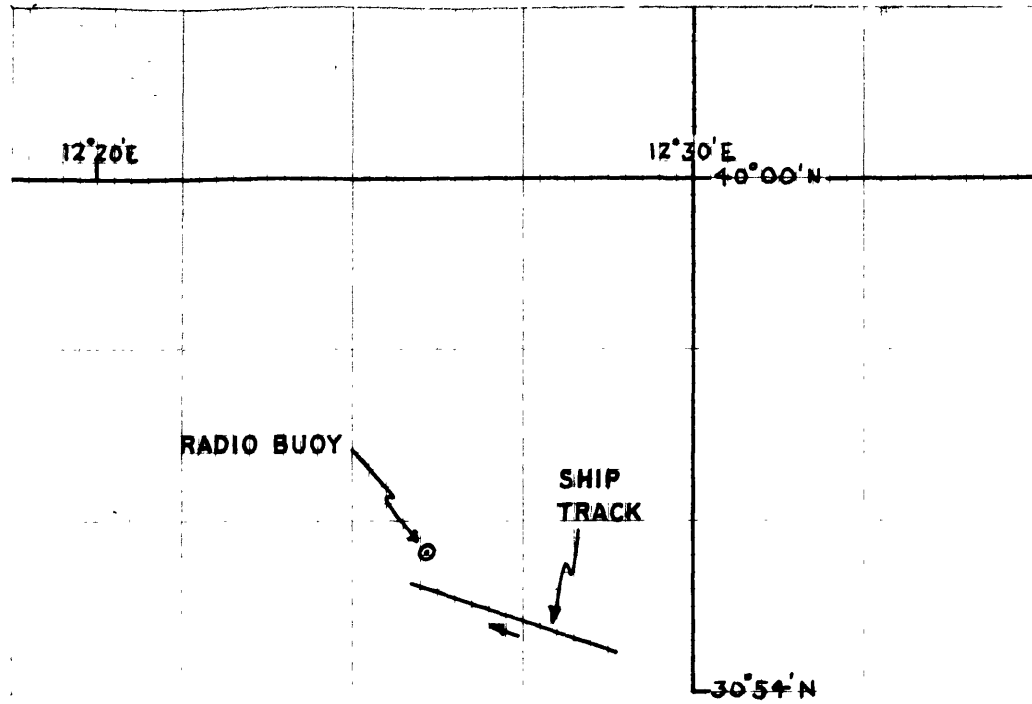


FIGURE 6

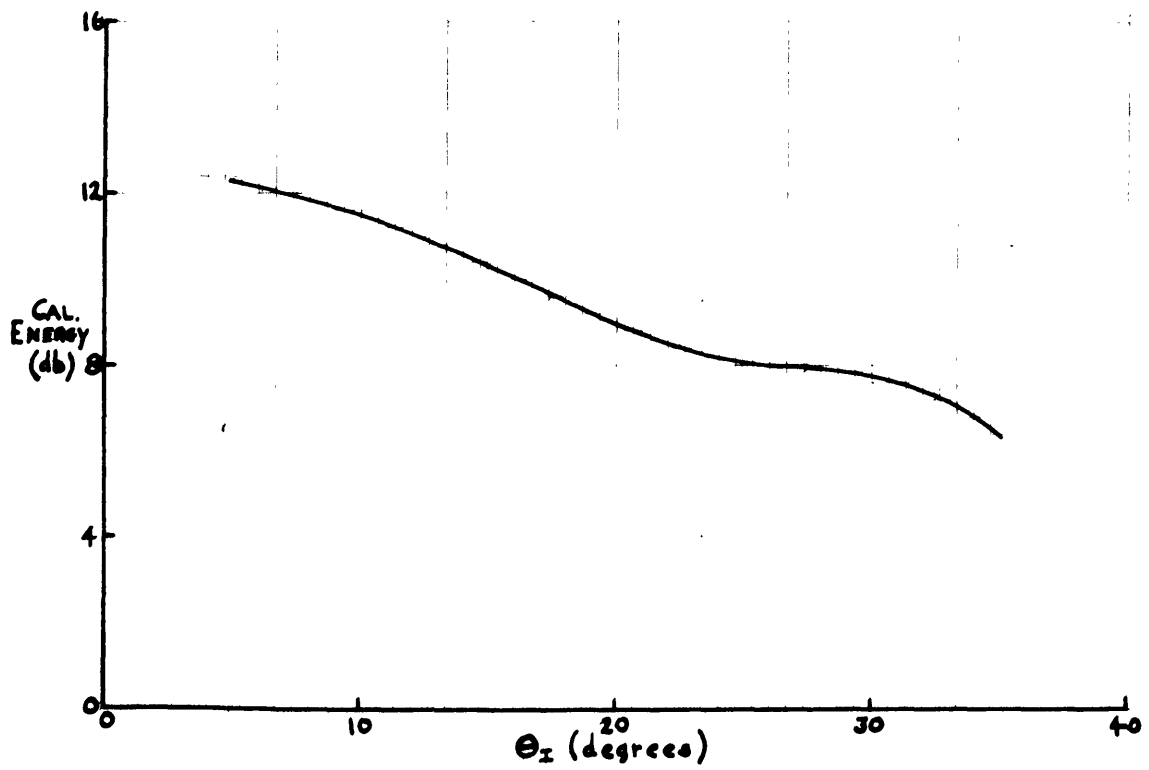


FIGURE 7

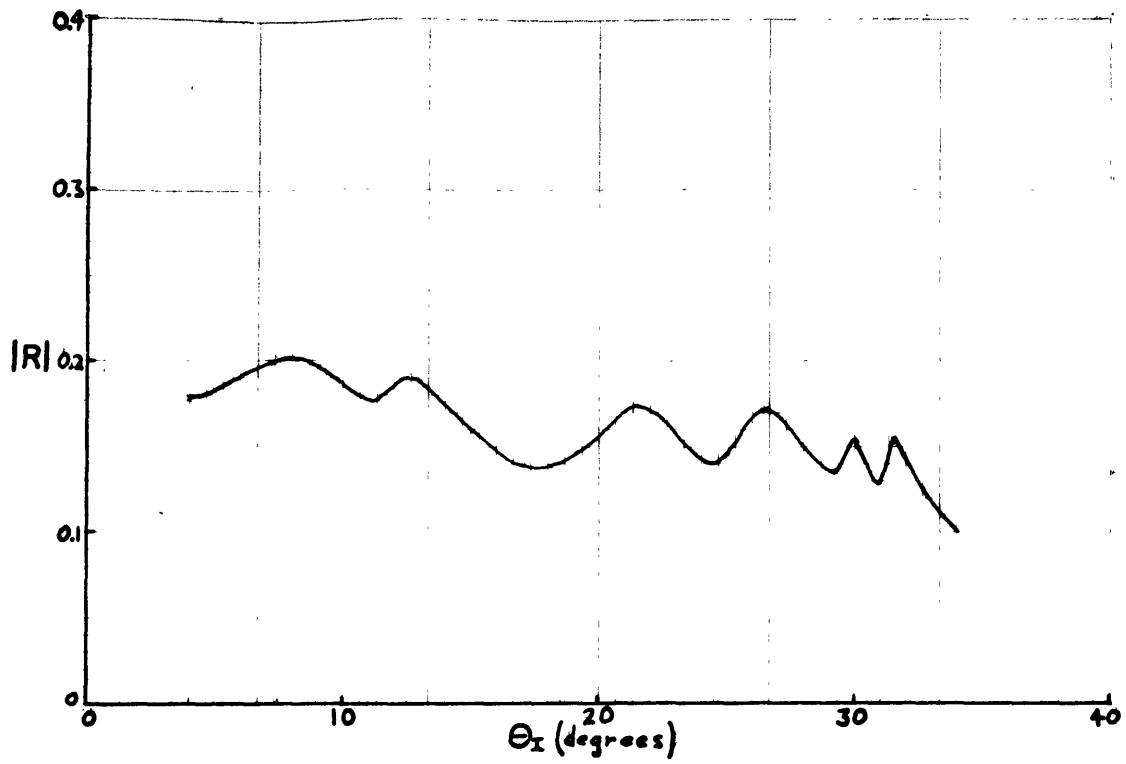


FIGURE 8

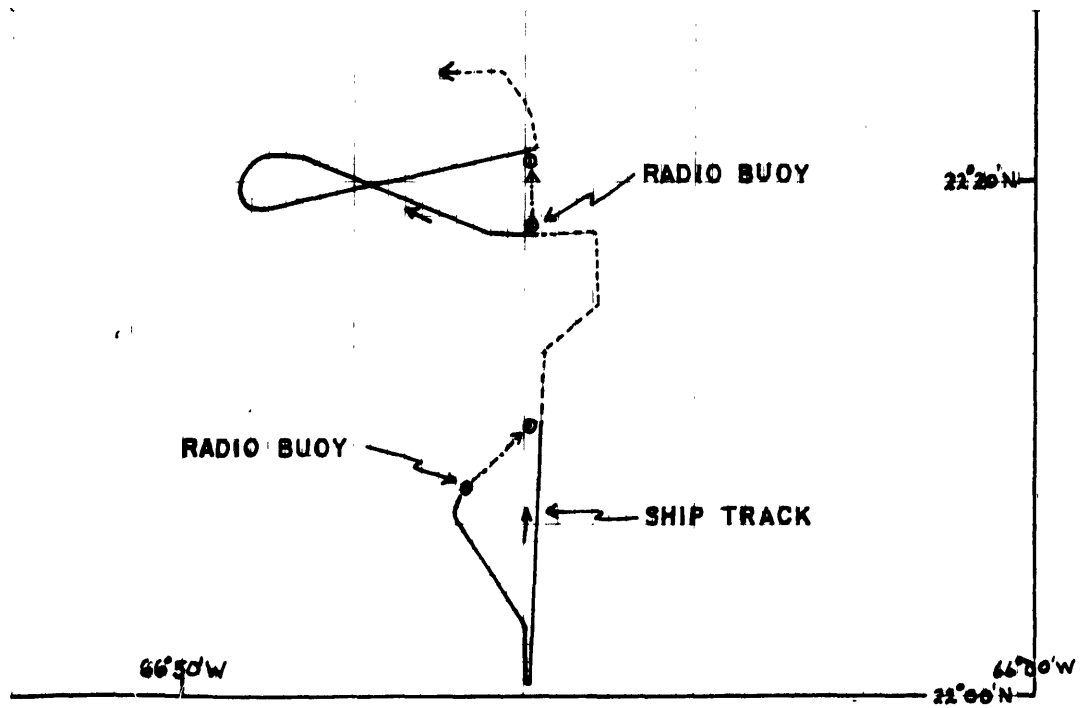


FIGURE 9

reflected energy at normal incidence, 2.) the depth of water and 3.) an estimation of the normal incidence reflectivity. It must be noted that we require a measurement of the source energy travelling in a downward direction so that the direct wave in the horizontal plane cannot be used for source energy calculations. It has been shown in part I-2 that normal incidence amplitude reflectivities for deep-sea sediments have a value remarkably close to 0.2, so that this figure has been used in the source energy calculations.

The variation of sound velocity with depth causes significant deviations of the ray path from a straight line for large angles of incidence (Officer, 1958 p.47). For angles of incidence less than 60 degrees however, the errors introduced are less than 1% so that the straight line approximation has been used.

Energy reflectivities are thus proportional to both the square of the ray path distance and the ratio of the measured reflected energy to the source energy. They are the square of the amplitude reflectivities. Ray path distances have been computed from the range between the ship and the radio buoy.

The five computed amplitude reflectivity graphs are shown in Figures 8, 12, 13, 14, and 15. They are each computed from hundreds of individual energy determinations which are corrected for radio transmission and spreading losses. Running median curves were drawn for the energy against  $\Theta_I$  graphs and these curves were then used to

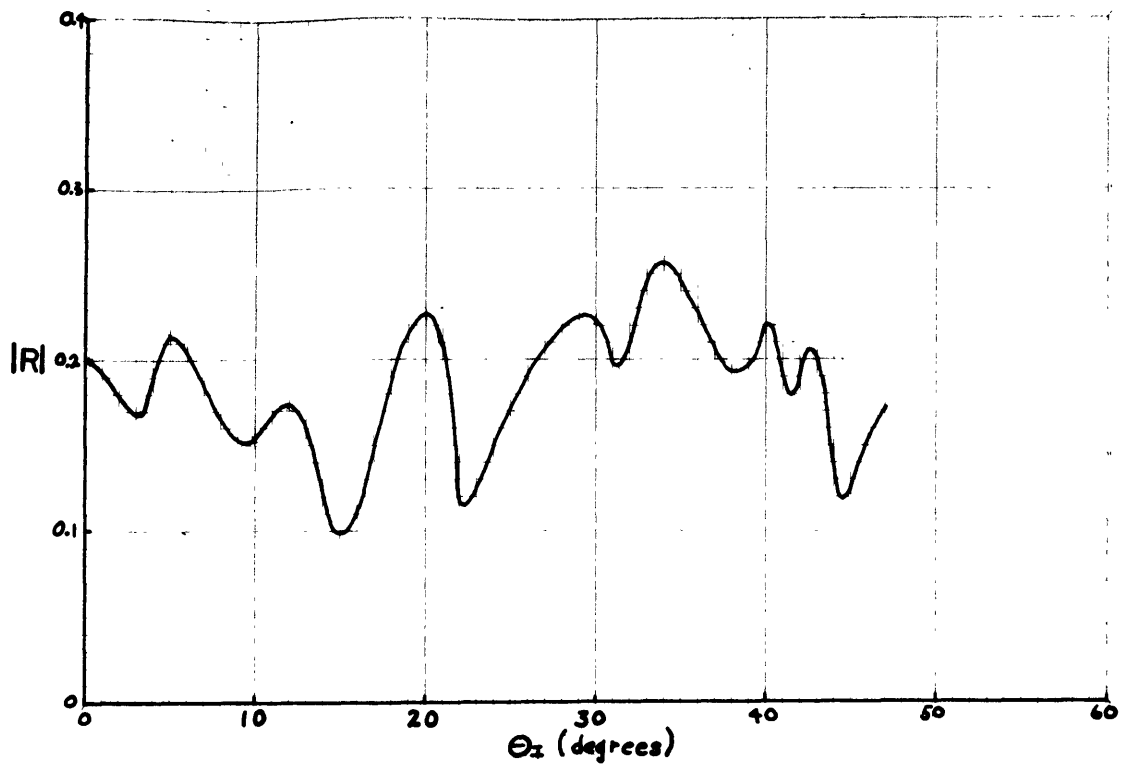


FIGURE 10

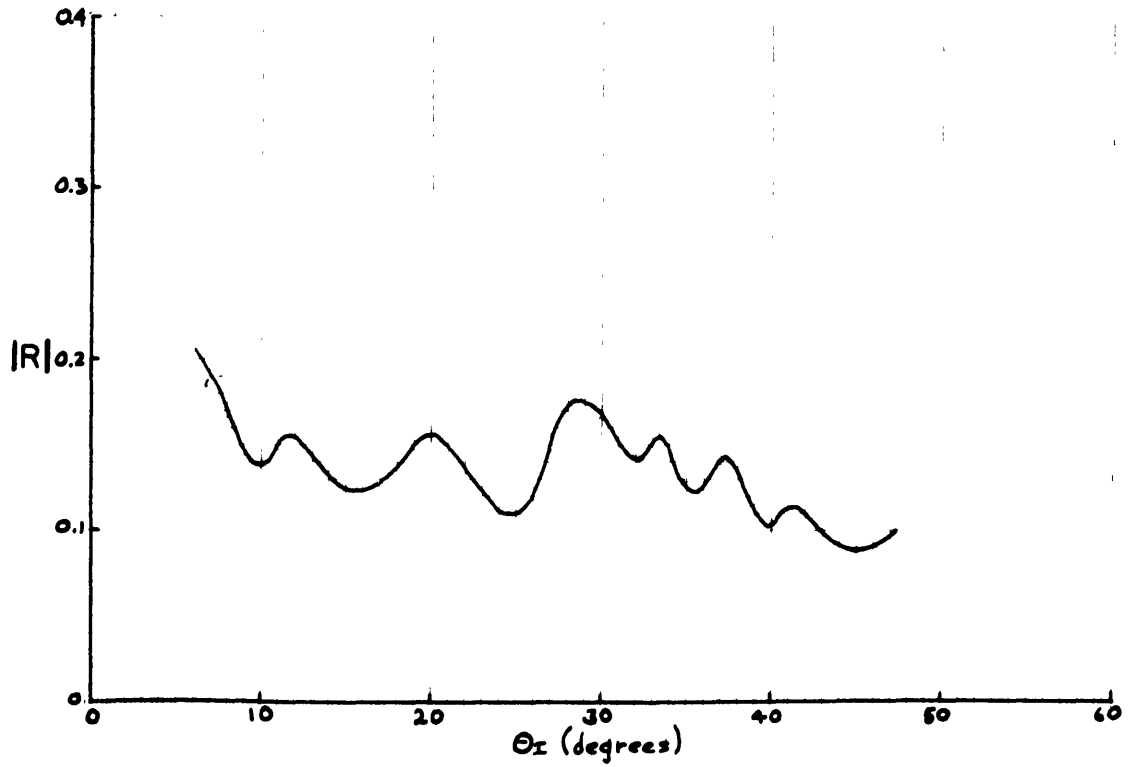


FIGURE 11

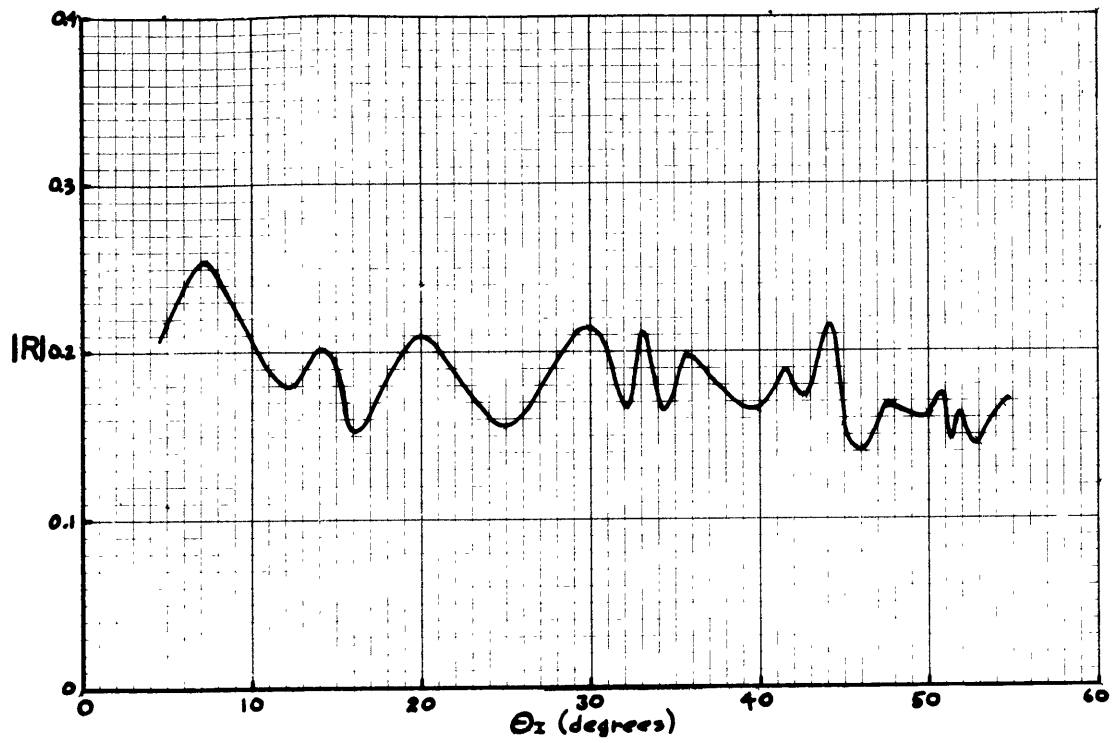


FIGURE 12

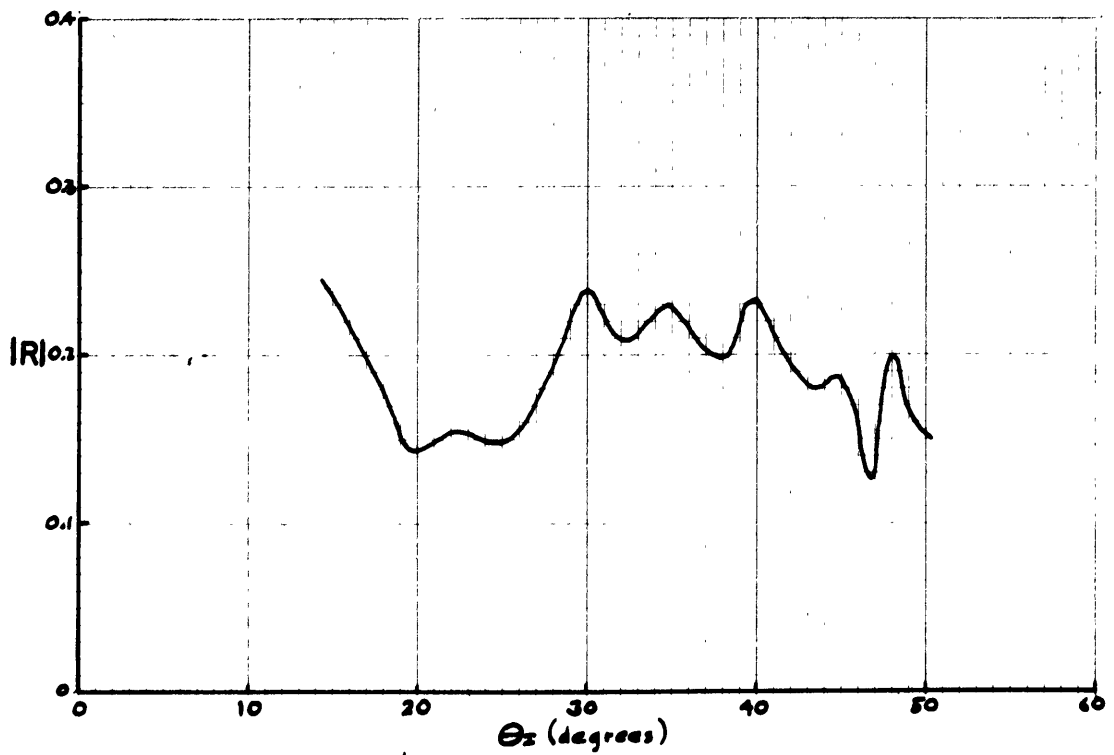


FIGURE 13



determine the energy and amplitude reflectivities.

In all cases, maxima and minima are clearly evident, as predicted in part I-3-b, and no appreciable increasing trend with angle of incidence is apparent. In the Tyrrhenian Sea there is a distinct downward trend with increasing angle of incidence.

Although it is difficult to say whether the curves will eventually bend downwards to an angle of intromission or upwards to a critical angle, it is possible to say that if a critical angle exists, that it will be greater than 60 degrees. From Figure 4, we can therefore conclude that the sound velocity of the in situ first layer sediments is less than 1.8 kilometers per second. From existing reflectivity curves for the case  $C_2 > C_1$ , amplitude reflectivities rise considerably at intermediate angles of incidence. It therefore appears that the Tyrrhenian Sea curve and possibly the combined Puerto Rico curves indicate the case  $C_2 < C_1$ , or a velocity inversion.

II-3

Conclusions

The measurement of oblique angle reflectivity of ocean sediments is an excellent method of measuring in situ sound velocities in the sediments. The experiments reported have made considerable progress in methods of continuous oblique angle profiling. The accurate measurement of the in situ sound velocity is, however, highly dependent on the determination of either the critical angle or the angle of intromission and thus it will be important in future experiments to obtain measurements at larger angles of incidence. This capability is dependent on range of transmission of the radio buoy, as well as depth of water.

The advantage of continuous profiling is that recording instruments on the ship can be used to indicate relative changes in reflectivity as the experiment progresses. On board the Chain, the precision graphic recorder was used with input data identical to that being recorded on the magnetic tape. The maxima and minima of the amplitude reflectivities shown in Figures 10-13 correlated well with the graphical results.

As the angle of incidence is increased in future experiments it will be important to make accurate measurements of the velocity-depth profile in the ocean as well as the normal incidence reflectivity. There is strong indication that such experiments will be highly successful in contributing to our knowledge and understanding of the characteristics of ocean sediments.

BIBLIOGRAPHY

Arons, A.B., and Yennie, D.R., 1950,  
Phase Distorsion of Acoustic Pulses Obliquely Reflected  
from a Medium of Higher Sound Velocity,  
J. Acoust. Soc. Am., v.22, p.231-237.

Ewing, W.M., Jardetzky, W.S., and Press, F., 1957,  
Elastic Waves in Layered Media,  
McGraw-Hill Inc., p.80.

Fry, J.C., and Raitt, R.W., 1961,  
Sound Velocities at the Surface of Deep Sea Sediments,  
J. Geop. Res., v.66, p.589-597.

Hamilton, E.L., 1956,  
Low Sound Velocities in High-Porosity Sediments,  
J. Acoust. Soc. Am., v.28, p.16-19.

Hill, M.N., 1952,  
Seismic Refraction Shooting in an Area of the Eastern  
Atlantic,  
Phil. Trans. Roy. Soc., London A, v.244, p.561-596.

Laughton, A.S., 1957.  
Sound Propagation in Compacted Ocean Sediments,  
Geophysics, v.22, p.233-260.

Officer, C.B., 1958,  
Introduction to the Theory of Sound Transmission,  
McGraw-Hill Inc.

Shumway, G., 1960,  
Sound Speed and Absorotion Studies of Marine Sediments  
by a Resonance Method,  
Geophysics, v.25, p.451-467.

Sutton, G.H., Berckheimer, H., and Nafe, J.E., 1957,  
Physical Analysis of Deep Sea Sediments,  
Geophysics, v.22, p.779-812.

Urlick, R.J., 1947,  
A Sound Velocity Method for Determining the Compressibility  
of Finely Divided Substances,  
J. Appl. Phys., v.18, p.983-987.

Wood, A.B., 1941,  
A Textbook of Sound,  
G. Bell and Sons, London.